

CELL AND TISSUE KINETICS

Edited by R. J. Berry

Volume 12, 1979

Editorial Board

M. Tubiana (*Chairman*), L. Simpson-Herren,
F. Bresciani, W. S. Bullough, A. B. Cairnie,
P. Dustin, J. I. Fabrikant, J. F. Fowler,
J. Fried, P. Galand, O. H. Iversen, S. Killmann,
L. G. Lajtha, C. P. Leblond, M. Lipkin,
M. L. Mendelsohn, D. Metcalf, N. Odartchenko,
H. M. Patt, M. F. Rajewsky, L. M. Schiffer,
G. G. Steel, F. A. Valeriote, A. J. Valleron,
D. W. van Bekkum, L. M. van Putten

Blackwell Scientific Publications
Oxford London Edinburgh Melbourne

CONTENTS

VOL. 12, NO. 1, JANUARY 1979

R. TICE, P. THORNE and E. L. SCHNEIDER. BISACK analysis of the phytohaemagglutinin induced proliferation of human peripheral lymphocytes	1
S. C. BARRANCO, W. E. BOLTON and J. K. NOVAK. A simple method for producing different growth fractions <i>in vitro</i> for use in anti-cancer drug studies	11
M. ROSENDAAL, G. S. HODGSON and T. R. BRADLEY. Organization of haemopoietic stem cells: the generation-age hypothesis	17
D. G. HIRST and J. DENEKAMP. Tumour cell proliferation in relation to the vasculature	31
T. LINDMO and E. O. PETERSEN. Delay of cell cycle progression after X-irradiation of synchronized populations of human cells (NH1K 3025) in culture	43
E. NISKANEN and M. J. CLINE. Growth of mouse and human bone marrow in diffusion chambers in mice. Development of myeloid and erythroid colonies and proliferation of myeloid stem cells in cyclophosphamide- and erythropoietin-treated mice	59
R. L. HUMPHREY, S. M. TREVIDI and CARMELITA G. FRONDOZA. Studies with murine LPC-1 plasmacytoma using [16- ¹⁴ C]arginine	71
G. R. CUNNINGHAM and CLAIRE HUCKINS. Failure to identify a spermatogonial chalone in adult irradiated testes	81
ELIZABETH HAMILTON. Diurnal variation in proliferative compartments and their relation to cryptogenic cells in the mouse colon	91
R.-M. BÖHMER. Flow cytometric cell cycle analysis using the quenching of 33258 Hoechst fluorescence by bromodeoxyuridine incorporation	101

VOL. 12, NO. 2, MARCH 1979

K. B. WOO. The discrete-time kinetic model analysis of DNA content distribution in experimental tumour cells	111
A. BRUNSTING, J. M. COLLINS, F. R. KANE and C. B. BAGWELL. An examination of some basic assumptions of DNA distribution analysis using biological data	123
O. P. F. CLAUSEN. Regenerative proliferation of mouse epidermal cells following application of a skin irritant (cantharidin): flow microfluorometric DNA measurements and [³ H]TdR incorporation studies of isolated basal cells	135
N. CHAUDAUDRA, J. M. RICHARD and E. P. MALAISE. Labelling index of human squamous cell carcinomas: comparison of <i>in vivo</i> and <i>in vitro</i> labelling methods	145
G. PIETU, N. MUNSCH, S. MOUSSET and C. FRAYSSINET. Effect of an inhibiting factor isolated from rat liver on DNA polymerases in regenerating rat liver	153

F. C. MONETTE and J. B. DEMELLO. The relationship between stem cell seeding efficiency and position in cell cycle	161
MARIA G. PALLAVICINI, A. M. COHEN, L. A. DETHLEFSEN and J. W. GRAY. <i>In vivo</i> effects of 5-fluorouracil and ftorafur[1-(tetrahydrofuran-2-yl)-5-fluorouracil] on murine mammary tumours and small intestine	177
A. M. ZAITOUN, I. LAUDER and W. A. AHERNE. Cell population kinetic profile of the mouse thymus, and the changes induced by prednisolone	191
ULLA MØLLER and J. K. LARSEN. DNA flow cytometry of isolated keratinized epithelia: a methodical study based on ultrasonic tissue disaggregation	203
N. JACOBSEN, H. E. BROXMEYER, E. GROSSBARD and M. A. S. MOORE. Colony-forming units in diffusion chambers (CFU-d) and colony-forming units in agar culture (CFU-c) obtained from normal human bone marrow: a possible parent-progeny relationship	213

VOL. 12, NO. 3, MAY 1979

G. ZAJICEK, Y. MICHAELI and J. REGEV. A new method for the estimation of cell cycle phases	229
SHIRLEY LEHNERT. Changes in growth kinetics of jejunal epithelium in mice maintained on an elemental diet	239
A. J. WALLE and M. R. PARAWARESCH. Estimation of effective eosinopoiesis and bone marrow eosinophil reserve capacity in normal man	249
O. VOS and INA J. C. WILSCHUT. Further studies on mobilization of CFUs	257
R. RADERMAN-LITTLE. The effect of temperature on the turnover of taste bud cells in catfish	269
S. E. AL-BARWARI and C. S. POTTEN. A cell kinetic model to explain the time of appearance of skin reaction after X-rays or ultraviolet light irradiation	281
N. M. BLACKETT and M. AGUADO. The enhancement of haemopoietic stem cell recovery in irradiated mice by prior treatment with cyclophosphamide	291
INA J. C. WILSCHUT, MIEKE E. ERKENS-VERSLUIS, R. E. PLOEMACHER, R. BENNER and O. VOS. Studies on the mechanism of haemopoietic stem cell (CFUs) mobilization. A role of the complement system	299
C. A. RUBIO, L. SKOOG and C. H. FOX. Viability of the cervical epithelium during carcinogenesis in mice	313
O. P. F. CLAUSEN, E. THORUD, R. BJERKNES and K. ELGJO. Circadian rhythms in mouse epidermal basal cell proliferation. Variations in compartment size, flux and phase duration	319
Book Reviews	339

VOL. 12, NO. 4, JULY 1979

P. H. FITZGERALD. Non-random association of mitotic cells from cultured human lymphocyte suspensions	341
--	-----

B. SCHULTZE, A. M. KELLERER and W. MAURER. Transit times through the cycle phases of jejunal crypt cells of the mouse. Analysis in terms of the mean values and the variances	347
A. HAGENBEEK and A. C. M. MARTENS. Functional cell compartments in a rat model for human acute myelocytic leukaemia	361
M.-N. LOMBARD, C. NADAL, B. FISZER-SZAFARZ, E. LE RUMMER and F. ZAJDELA. Interference of sex-related factors in the response of liver cells to experimental mitotic stimuli	379
S. ZUCKER, MIRIAM S. MICHAEL, RITA M. LYSIK, M. J. GLUCKSMAN, J. REESE, A. RUDIN and J. DiSTEPHANO. Lipoprotein inhibitor of bone marrow cells in tumor-bearing rats	393
R. P. WILLIAMS, I. L. CAMERON and E. K. ADRIAN. Effects of intestinally absorbed thymidine on tritiated thymidine utilization	405
R. M. KLEIN. Alteration of neonatal rat parotic gland acinar cell proliferation by guanethidine-induced sympathectomy	411
MARGARET J. IRONS and Y. CLERMONT. Spermatogonial chalone(s): effects on the phases of the cell cycle of type A spermatogonia in the rat	425
E. O. RIJKE and R. E. BALLIEUX. Thymus derived inhibitor of lymphocyte proliferation. I. Isolation and assessment of tissue specificity	435
I. L. CAMERON, MARY R. H. POOL and T. R. HOAGE. Low level incorporation of tritiated thymidine into the nuclear DNA of Purkinje neurons of adult mice	435

VOL. 12, NO. 5, SEPTEMBER 1979

G. ZAJICEK, Y. MICHAELI and J. REGEV. On the progenitor cell migration velocity	453
M. R. ALISON and N. A. WRIGHT. Testosterone-induced cell proliferation in the accessory sex glands of mice at various times after castration	461
M. R. ALISON and N. A. WRIGHT. Differential lethal effects of both cytosine arabinoside and hydroxyurea on jejunal crypt cells and testosterone-stimulated accessory sex glands	477
KAREN K. FU and G. G. STEEL. Growth kinetics of a rat mammary tumour transplanted into immune-suppressed mice	493
S. SKOG, E. ELIASSON and EVA ELIASSON. Correlation between cell size and position within the division cycle in suspension cultures of Chang liver cells	501
H. K. AWWAD, M. HEGAZY, S. EZZAT, N. EL-BOLKAINY and M. V. BURGERS. Cell proliferation of carcinoma in Bilharzial bladder: an autoradiographic study	513
G. WAGEMAKER, M. F. PETERS and S. J. L. BOL. Induction of erythropoietin responsiveness <i>in vitro</i> by a distinct population of bone marrow cells	521
R. E. PLOEMACHER, P. L. VAN SOEST, G. WAGEMAKER and E. VAN'T HULL. Particle-induced erythropoietin-independent effects on erythroid precursor cells in murine bone marrow	539
H.-E. WICHMANN, M. D. GERHARDTS, H. SPECHTMEYER and R. GROSS. A mathematical model of thrombopoiesis in rats	551

W. R. HANSON, R. J. M. FRY and A. R. SALLESE. Cytotoxic effects of colcemid or high specific activity tritiated thymidine on clonogenic cell survival in B6CF ₁ mice	569
U. MØLLER, N. R. HARTMANN and M. FABER. Mitotic index, influx and mean transit time in the hamster cheek pouch epithelium, a partially synchronized cell system. Presentation of a mathematical model based on a non-stationary probability density function for the transit time in a compartment	581
N. CHAUDAUDRA and E. P. MALAISE. <i>In vitro</i> incorporation of [³ H]TdR in human and murine solid tumours. Influence of 5-fluorouracil and/or hyperbaric oxygen on spatial distribution of labelling	597
P. DAVISON, S. LIU and M. KARASEK. Limitations in the use of [³ H]thymidine incorporation into DNA as an indicator of epidermal keratinocyte proliferation <i>in vitro</i>	605
EDNA B. LAURENCE, D. J. SPARGO and A. L. THORNLEY. Cell proliferation kinetics of epidermis and sebaceous glands in relation to chalone action	615
P. V. BYRNE, HILDEGARD HEIT and W. HEIT. Buoyant density analysis of myeloid colony-forming cells in germfree and conventional mice	635
R. M. KLEIN. Analysis of intestinal cell proliferation after guanethidine-induced sympathectomy. II. Percentage labelled mitoses studies	649
Brief Communication	
R. VAN WIJK and K. W. VAN DE POLL. Variability of cell generation times in a hepatoma cell pedigree	659
PROCEEDINGS OF THE CELL KINETICS SOCIETY. Third Annual Meeting, March 15–17, 1979, Hotel Four Ambassadors, Miami, Florida, U.S.A.	665
Author Index to Volume 12	691

TRANSIT TIMES THROUGH THE CYCLE PHASES
OF JEJUNAL CRYPT CELLS OF THE MOUSE
ANALYSIS IN TERMS OF THE MEAN VALUES AND THE
VARIANCES

B. SCHULTZE, A. M. KELLERER AND W. MAURER

Institut für Medizinische Strahlenkunde der Universität Würzburg, Germany

(Received 27 February 1978, revision received 1 September 1978)

ABSTRACT

Mean transit times as well as variances of the transit times through the individual phases of the cell cycle have been determined for the crypt epithelial cells of the jejunum of the mouse. To achieve this the fraction of labelled mitoses (FLM) technique has been modified by double labelling with [³H] and [¹⁴C]thymidine. Mice were given a first injection of [³H]thymidine, and 2 hr later a second injection of [¹⁴C]thymidine. This produces a narrow subpopulation of purely ³H-labelled cells at the beginning of G₂-phase and a corresponding subpopulation of purely ¹⁴C-labelled cells at the beginning of the S-phase. When these two subpopulations progress through the cell cycle, one obtains FLM waves of purely ³H- and purely ¹⁴C-labelled mitoses. These waves have considerably better resolution than the conventional FLM-curves. From the temporal positions of the observed maxima the mean transit times of the cells through the individual phases of the cycle can be determined. Moreover one obtains from the width of the individual waves the variances of the transit times through the individual phases. It has been found, that the variances of the transit times through successive phases are additive. This indicates that the transit times of cells through successive phases are independently distributed. This statistical independence is an implicit assumption in most of the models applied to the analysis of FLM curves, however there had previously been no experimental support of this assumption. A further result is, that the variance of the transit time through any phase of the cycle is proportional to the mean transit time. This implies that the progress of the crypt epithelial cells is subject to an equal degree of randomness in the various phases of the cycle.

A number of authors have developed computer programs for the analysis of fraction labelled mitoses (FLM) curves obtained after application of [³H]thymidine (see for example Steel & Hanes (1970), Takahashi *et al.* (1971), Brockwell *et al.* (1972), Gilbert (1972), Ashihara

Correspondence: Professor Dr B. Schultze, Institut für Med. Strahlenkunde der Universität Würzburg, Versbacher Landstrasse, 5, 8700 Würzburg, Federal Republic of Germany.

0008-8730/79/0700-0347\$02.00 © 1979 Blackwell Scientific Publications

(1973), and Hartmann *et al.* (1975)). These algorithms require the *a priori* assumption of a particular analytical form of the distribution of transit times through the cell cycle and its phases (e.g. normal, log-normal, or gamma-distribution). They are also based on the presumption that the transit times through successive phases are independently distributed. With these assumptions the computer methods permit a derivation of mean transit times through the cycle and its phases. The computer algorithms produce also estimated values of the variances of the transit times for the individual phases; however, these estimates are subject to considerable uncertainties, and little information on the variances has been obtained in past investigations.

The present study utilizes the FLM method modified by double labelling with [³H] and [¹⁴C]thymidine. This double labelling method leads to maxima of purely ³H- and purely ¹⁴C-labelled mitoses which are much sharper than those obtained in the usual way after single injection of [³H]thymidine. Accordingly, as will be seen, no sophisticated mathematical methods are necessary for the derivation of the mean transit times and of the variances of the transit times from these curves. Also it will be unnecessary to postulate an analytical form of the distributions of transit times.

The experiments have been performed on the crypt epithelial cells of the jejunum of the mouse. The results permit an answer to the question of additivity of the variances of the transit times through successive phases of the cycle. This, in turn, leads to a statement on the correlation, or lack of correlation of transit times of a cell through successive phases.

MATERIALS AND METHODS

Animals

Sixty-eight male mice of the NMRI strain (Zentralinstitut für Versuchstierzucht, Hannover) with an average weight of 33 g and about 3 months old were used. The animals received standard diet Altromin R and water *ad libitum*, and were housed in a temperature controlled animal room at 23°C with light from 06.00 to 18.00 hours.

Labelled thymidine

Thymidine-methyl-³H ([³H]TdR; 6.7 Ci/mmol) and thymidine-2-¹⁴C ([¹⁴C]TdR; 43.7 mCi/mmol or 54.1 mCi/mmol) were obtained from New England Nuclear Chemicals, U.S.A.

Squashes of isolated crypts

A piece of jejunum, 6 cm from the pylorus, was removed and fixed in acetic acid-ethanol (1:3) for 24 hr and then Feulgen stained (hydrolysis in 1 N HCl at 60°C for 6 min). Individual crypts were isolated and squashed (for details see Schultze *et al.*, 1972).

Double layer autoradiography of the crypt squashes

The slides with the squashed crypts were dipped into diluted Ilford K2 emulsion (1:1 with water). After 6–12 days exposure the autoradiographs were developed with amidol developer, dried, dipped into a 10% gelatin solution, dried overnight, dipped into a 20% formalin solution for hardening (20 min) and rinsed in water (10 min). A thick layer of Ilford K2 emulsion (about 20 μm thick after development) was then spread onto the slides. After a 21–28 day exposure period the slides were developed and covered with a cover slip.

The grains in the first, thin emulsion layer represent the ^3H -label and the tracks in the second, thick emulsion layer the ^{14}C -label. With an appropriate ratio of [^3H]TdR to [^{14}C]TdR activity the differently labelled interphase cells or mitoses can be discriminated. For details see Schultze *et al.* (1976).

The mice received a first i.p. injection of [^3H]TdR (1 $\mu\text{Ci/g}$) in 0.3 ml physiological saline and a second i.p. injection 2 hr later of [^{14}C]TdR (0.06 $\mu\text{Ci/g}$) in 0.2 ml physiological saline. Two animals each were killed by decapitation every hr up to 30 hr after the first [^3H]TdR injection. On double layer autoradiographs (Schultze *et al.*, 1976) of the slides containing the squashed crypts the numbers of purely ^3H - and purely ^{14}C -labelled mitoses relative to all mitoses were determined as a function of the time after double labelling.

The modification of the fraction of labelled mitoses method proposed by Maurer and co-workers (Maurer *et al.*, 1972; Schultze *et al.*, 1972) replaces the single injection of [^3H]TdR by a double labelling with [^3H]- and [^{14}C]TdR. The midpoint between ^3H - and ^{14}C -labelling will be considered as time zero. Mice receive at first injection of [^3H]TdR at time $t = -1$ hr and a second injection of [^{14}C]TdR 2 hr later at time $t = 1$ hr. This procedure has the result that all those cells are purely ^3H -labelled that have left S-phase in the time interval $t = -1$ hr to $t = +1$ hr; all those cells are purely ^{14}C -labelled that have entered S-phase in this time interval.

Since the crypt as a whole represents a steady state system with constant cell density throughout the cycle, the number of purely ^3H -labelled and of purely ^{14}C -labelled cells should be equal. The cell flux in the jejunal crypt of the mouse is 5.5% of all crypt cells per hour (Schultze *et al.*, 1972). Therefore, a crypt with about 200 cells contains on the average twenty-two purely ^3H - and twenty-two purely ^{14}C -labelled cells. According to the mitotic duration of about 0.5 hr the crypt contains on the average 5.5 mitoses.

RESULTS

Fig. 1 depicts the measured FLM curves of the purely ^3H -labelled mitoses and those of the purely ^{14}C -labelled mitoses. The double labelling results in relatively narrow cohorts of purely ^3H - and purely ^{14}C -labelled cells. Accordingly the resolution of the individual mitotic peaks is much better than in experiments with a single injection of [^3H]TdR. The first peak (1) corresponds to the purely ^3H -labelled cells that have passed through G_2 and are observed as purely ^3H -labelled mitoses during the subsequent mitosis. Peak (3) represents the same cohort of cells after passage through an additional entire cell cycle. After passage through another complete cell cycle these cells form peak (5).

In contrast to the purely ^3H -labelled cells the purely ^{14}C -labelled cells must first pass through S; after passage through G_2 they then form the first peak of purely ^{14}C -labelled mitoses (2). Peak (4) consists of the same group of cells after passage through a further complete cell cycle.

Mean values and variances of the transit times

In the usual FLM experiment with a single injection of [^3H]TdR one obtains a curve which is the superposition of consecutive waves of labelled mitoses that are not always clearly separated but can have substantial overlap. Suitable numerical methods can then be applied to resolve the individual waves and to compute the underlying distributions of transit times

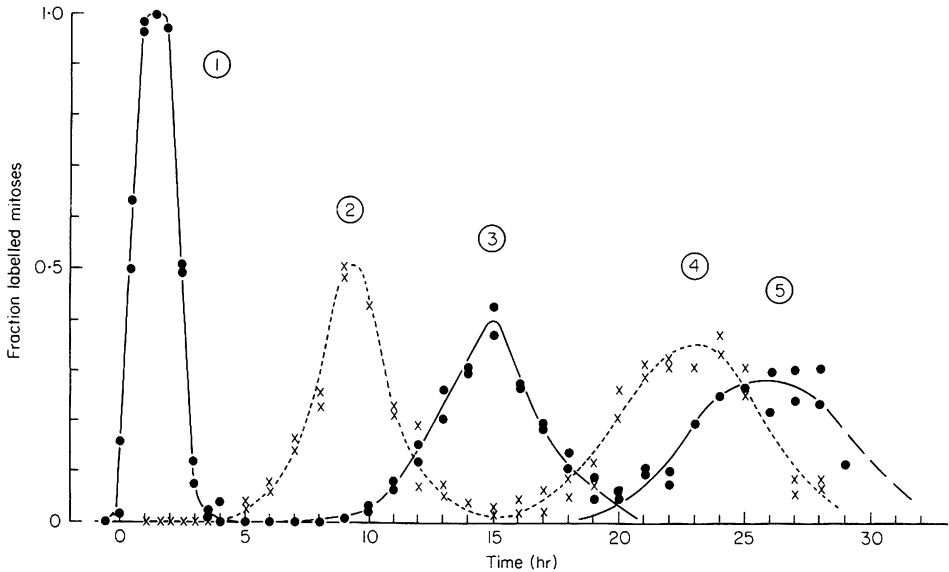


FIG. 1. Fraction of purely ^3H - (●) and purely ^{14}C -labelled (x) mitoses as a function of time after double labelling. The midpoint between ^3H - and ^{14}C -labelling is taken as time zero. Solid line indicates curves adjusted to ^3H -data; dotted lines are curves adjusted to ^{14}C -data.

through the different phases of the cell cycle. In contrast the double-label FLM curve consists of well separated waves of purely ^3H - and purely ^{14}C -labelled mitoses. Accordingly no mathematical procedure for the resolution of the individual waves is required.

In the following, the analysis is further simplified since only the mean values and the variances of the individual waves of labelled mitoses (1, 2, 3, 4, in Fig. 1) will be utilized. From these parameters the mean transit times and the variances of the transit times for the individual phases of the cell cycle will be derived. Before this analysis is presented some formal definitions are necessary and certain relations between the mean values and the variances of the probability distributions will have to be considered.

The mean transit times through G_1 , S, G_2 , mitosis and through the whole cycle (C) will in the following be designated by \bar{t}_{G_1} , \bar{t}_S , \bar{t}_{G_2} , \bar{t}_M and \bar{t}_C . The actual transit time of an individual cell through one of the phases of the cycle is, however, a random variable which may differ substantially from the mean value of the transit time for this phase. The distributions of values which actually occur must therefore be described by probability densities. These densities will be designated by $f_{G_1}(t)$, $f_S(t)$, $f_{G_2}(t)$ and $f_C(t)$. They are defined in the usual way. For example $f_S(t) dt$ is the probability that a cell needs a time between t and $t + dt$ to traverse the S-phase. The variances of the transit times which belong to the individual densities will be designated by $\sigma_{G_1}^2$, σ_S^2 , $\sigma_{G_2}^2$, and σ_C^2 . For simplicity, it will be assumed that the duration of mitosis is constant and, as shown in earlier work (Burholt *et al.*, 1973), equal to 0.5 hr.

It can be shown that the mean transit time through the whole cycle is equal to the sum of the mean transit times through the individual phases of the cycle regardless whether the transit times through successive phases are independent or not. For the variances the situation is more complicated. The variances are additive only if the transit times through successive phases are uncorrelated. Absence of correlation is a condition in the commonly applied

theoretical models of cell kinetics that postulate independently distributed transit times through the cycle phases. For uncorrelated transit times only one obtains:

$$\sigma_{S+G_2}^2 = \sigma_S^2 + \sigma_{G_2}^2, \quad \text{or} \quad \sigma_C^2 = \sigma_{G_1}^2 + \sigma_S^2 + \sigma_{G_2}^2 \tag{1}$$

The small term σ_M^2 is omitted because, as stated above, fluctuations of transit time through mitosis will be neglected.

If there is correlation between the transit times of a cell through successive phases of the cycle, the variance of the total transit time will be larger than the sum of the variances for the individual phases. In fact, one can show that under certain assumptions and in the limiting case of complete correlation the standard deviations, not the variances, are additive:

$$\sigma_C = \sigma_{G_1} + \sigma_S + \sigma_{G_2} \tag{2}$$

These considerations will be applied in the following. The evaluation of the variances of the FLM curves in Fig. 1 will lead to the conclusion that equation 1, not equation 2, applies. This implies that there is no significant correlation between transit times of a cell through successive phases of the cycle.

The individual mitotic waves which are labelled as curves 1–5 in Fig. 1 correspond to the distributions (1) $f_{G_2}(t)$, (2) $f_{S+G_2}(t)$, (3) $f_{C+G_2}(t)$, (4) $f_{C+S+G_2}(t)$, and (5) $f_{2C+G_2}(t)$ (see Table 1). For example wave (1) corresponds to the distribution of transit times of individual cells through G_2 ; similarly wave (3) corresponds to the distribution of transit times of individual cells through G_2 and the entire subsequent cycle, and so on. The agreement between the observed waves 1–5 and the distributions of transit times ($f_{G_2}(t)$ etc.) is however incomplete because of the finite initial width of the labelled population in phase age (2 hr) and the finite duration of mitosis (0.5 hr). In the appendix, a formula is derived which gives the relation between the distributions of transit times and the FLM curves actually observed. The essential result is that the mean values and the variances of the transit time distributions can readily be obtained by numerical integration of the FLM curves. The values thus obtained are listed in Table 1. The mean transit time obtained from the FLM wave i is designated as \bar{t}_i , the variance

TABLE 1. Mean values and variances obtained from the waves of labelled mitoses in Fig. 1 by numerical integration*

Mitotic wave	Transit through phases	Area (hr)	Mean transit time \bar{t}_i (hr)	Variance σ_i^2 (hr ²)	Standard deviation σ^2 (hr)	σ_i^2/\bar{t}_i (hr)
(1)	$G_2 + \frac{M}{2}$	1.94	1.56	(0.14)	0.37	(0.1)
(2)	$S + G_2 + \frac{M}{2}$	1.88	9.37	2.82	1.68	0.30
(3)	$C + G_2 + \frac{M}{2}$	1.97	14.84	4.11	2.03	0.28
(4)	$S + C + G_2 + \frac{M}{2}$	2.4	22.68	6.49	2.55	0.29
(5)	$2C + G_2 + \frac{M}{2}$	(2.28)	(26.0)	(8.28)		(0.32)

* See equations (A.6) and (A.7)

obtained from the FLM wave i is designated as σ_i^2 . In addition the areas under the curves are listed. Since these numerical values are obtained by numerical integrations over the interpolated curves in Fig. 1, they are subject to a degree of uncertainty. This uncertainty is relatively small for the areas and for the mean values. For the variances it is larger because these are influenced substantially by the tails of the distributions and these tails are subject to the largest statistical errors.

The data given for wave (5) are quite uncertain since only one half of this wave has been observed; the dashed part of the curve is a mere estimate based on the assumption that the area under the curve is roughly equal to that theoretically expected. The mean value and variance for curve (5) are therefore put in parentheses in Table 1.

The area under each of the waves of labelled mitoses should be equal to 2 hr (see appendix); the values actually obtained are close to 2 hr for waves (1), (2), and (3). For wave (4) the area is somewhat too large; this may be due to the difficulty of distinguishing true labelling from spurious labelling of mitoses at times when the label in the cell is already diluted by two successive mitoses.

TABLE 2. Mean values and variances of the transit times through individual phases of the cell cycle

Phase	Mean \bar{i} (hr)	Variance σ^2 (hr ²)	Coefficient of variation	
			σ/\bar{i}	σ^2/\bar{i} (hr)
G ₁ Phase	3.7	1.2 (1.1)	0.30 (0.27)	0.32
S Phase	7.8	2.7 (2.3)	0.21 (0.19)	0.34
G ₂ Phase	1.3	0.16 (0.34)	0.31 (0.46)	0.12
Mitosis	0.5	— (0.15)	— (0.8)	—
Entire Cycle	13.3	4.0 (4.0)	0.15 (0.15)	0.30

The values in brackets correspond to the relation: $\sigma^2 = 0.29 \text{ hr} \cdot \bar{i}$.
The variance for G₂ is listed but it is subject to considerable uncertainty.

Numerical evaluation of the mean values and the variances

From the values listed in Table 1 one obtains the mean transit times through the individual phases of the cycle and through the whole cycle that are listed in Table 2. The agreement of the values in Table 2 with the experimental results is illustrated in Fig. 2. The lengths of the horizontal bars represent the mean transit times observed for the individual FLM waves. It is readily seen that the experimental data contain an internal check insofar as the same duration of the whole cycle (13.3 hr) is obtained from a comparison of waves 3 and 1 and waves 4 and 2, and the same duration of S-phase (7.8 hr) is obtained from a comparison of waves (2) and (1) and waves (4) and (3).

The variances σ_i^2 that are obtained from the observed waves of labelled mitoses (see Table 1) are plotted against the corresponding mean transit times \bar{i}_i in Fig. 3. These values permit an answer to the question whether the transit times of a cell through successive phases of the cycle, or through successive cycles, are correlated. As pointed out, complete correlation corresponds to additivity of the standard deviations σ_i , while lack of correlation corresponds to additivity of the variances σ_i^2 . One may consider pairs of observed curves $f_i(t)$ which differ by the same phase interval. If one finds equal increments of the variance in such pairs, the

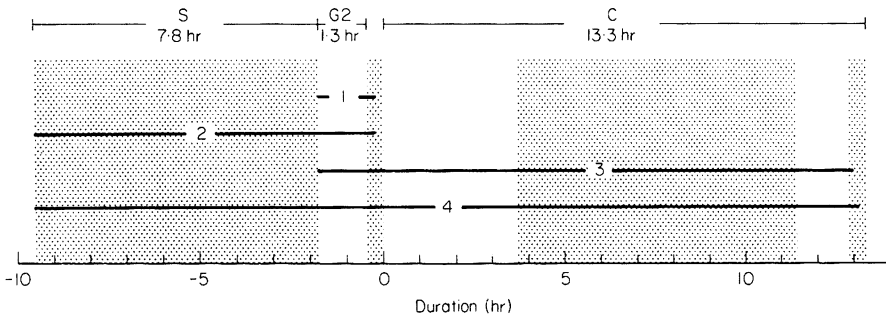


FIG. 2. Representation of the mean transit times \bar{t}_i obtained from waves (1) to (4) of labelled mitoses.

The shaded areas represent S-phase and mitosis. The length of the phases indicated in the diagram correspond to the mean transit times given in Table 2. The lengths of the horizontal bars correspond exactly to the values \bar{t}_i derived by numerical integration from the FLM waves (see Table 1).

variance is additive. If, on the other hand, one finds equal increments of the standard deviations, the standard deviations are additive.

Wave (2) and (1) and wave (4) and (3) differ by the same phase interval, namely S-phase, and the differences of the variances are in the two cases approximately the same:

$$\sigma_2^2 - \sigma_1^2 = 2.7 \text{ hr}^2 \quad \text{and} \quad \sigma_4^2 - \sigma_3^2 = 2.4 \text{ hr}^2 \quad (3)$$

The differences in the standard deviations are, on the other hand, substantially unequal:

$$\sigma_2 - \sigma_1 = 1.31 \text{ hr} \quad \text{and} \quad \sigma_4 - \sigma_3 = 0.5 \text{ hr} \quad (4)$$

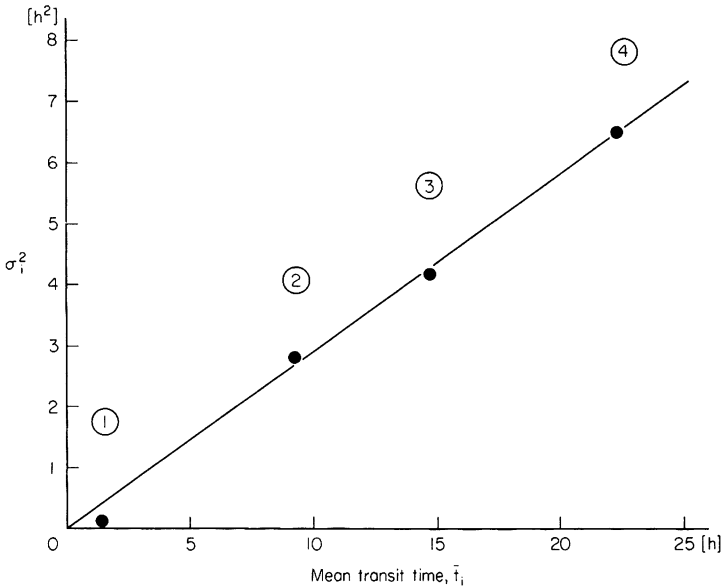


FIG. 3. Relation between the variances σ_i^2 and the mean transit times \bar{t}_i obtained from the four peaks of labelled mitoses in Fig. 1.

The straight line corresponds to the relation: $\sigma_i^2 = 0.29 \text{ hr} \cdot \bar{t}_i$. The values for σ_i^2 and \bar{t}_i are listed in Table 1.

Similarly wave (3) and (1) and wave (4) and (2) differ by the interval of an entire cycle C . Again the differences of the variances are nearly the same:

$$\sigma_3^2 - \sigma_1^2 = 4 \text{ hr}^2 \quad \text{and} \quad \sigma_4^2 - \sigma_2^2 = 3.7 \text{ hr}^2 \quad (5)$$

while the differences between the standard deviations are markedly unequal:

$$\sigma_3 - \sigma_1 = 1.7 \text{ hr} \quad \text{and} \quad \sigma_4 - \sigma_2 = 0.9 \text{ hr} \quad (6)$$

These results are consistent with equations (3) and (5) rather than with equations (4) and (6); accordingly, the variances, not the standard deviations, are additive. One concludes that there is, in the present experiment, no significant correlation between the transit times of a cell through successive phases. In other words, the experimental observations are in agreement with the assumption that the transit times vary randomly among the jejunal crypt cells. At least for this particular cell system it is therefore justified to disregard statistical correlation between the durations of successive phases for individual cells.

The conclusion that the variances are additive permits the derivation of their numerical values for the individual phases of the cycle. This derivation is quite analogous to the determination of the mean transit times from the values \bar{t}_i . The values for the S-phase and for the entire cycle are obtained from Equations (3) and (5). The value for G_2 -phase is set equal to the variance obtained from wave (1) of labelled mitoses; however, this value may, as pointed out in the appendix, be subject to considerable inaccuracy. The value for G_1 -phase results as the difference between the variance for the entire cycle and the sum of the variances for S-phase and G_2 -phase; as stated earlier, the variance of transit times through mitosis is disregarded. The results are listed in Table 2.

TABLE 3. Cycle phase durations of crypt cells in the small intestine of the mouse

Region of small intestine	Duration of the cycle phases (hr)					Authors
	T_{G1}	T_S	T_{G2}	T_M	T_C	
Lower ileum	9.5	7.5	0.5-1.0	0.45	18.75	Quastler & Sherman (1959)
Duodenum	4.5-5.5	5		<2	11.5-15.5	Leshner <i>et al.</i> (1961)
Upper small intestine*	4.7	6.7	0.9	0.6	13.1	Leshner & Sacher (1968)
Jejunum	3.2	8.3	0.75	0.9	13.1	Sigdestad & Leshner (1972)
Jejunum		7.4†			16.0	Kovacs & Potten (1973)
Upper jejunum	3.66	7.61	1.15	—	12.42	
Upper jejunum				0.86	11.8	Al-Dewachi <i>et al.</i> (1975)
Jejunum				0.5		Burholt <i>et al.</i> (1973)
Jejunum	4.5	8.0	1.0	0.52-0.54	14.0	Schultze <i>et al.</i> (1972)
Jejunum	3.7	7.8	1.3		13.3	Present work

* For 100 day old mice.

† Mean of seventeen published values for the mouse.

DISCUSSION

The analysis of the FLM curves is based on the implicit assumption that the kinetic parameters of the epithelial cells are identical throughout the proliferating region of the crypt. Cairnie *et al.* (1965) have, in their thorough study of the epithelial cells of the jejunum of the

rat, shown that the durations of the cycle and of its different phases are nearly the same between the bottom and the top of the crypt. Only the first cell positions at the bottom of the crypt are an exception; in the first positions cycle times have been found which were larger than those in the rest of the crypt. Al-Dewachi *et al.* (1975) have performed stathmokinetic experiments on the jejunum of the mouse with vincristine. These authors come to the conclusion that the proliferation in the crypt of the mouse corresponds closely to that in the rat. The results obtained in the present article are also a strong indication that cell proliferation is homogeneous within the crypt of the mouse. If the proliferation was non-uniform, one could not obtain the excellent agreement between the cycle times and the S phase durations which have been obtained from the waves of purely ^3H -labelled mitoses, on the one hand, and purely ^{14}C -labelled mitoses, on the other hand. It has been stated that wave (5) in Fig. 1 appears about 2 hr earlier than expected from the analysis of the first four waves. It may be noted that this cannot be due to the somewhat slower proliferation of the cells at the bottom of the crypts. If the mitotic wave (5) was due mainly to progeny of cells which, at the time of labelling, were near the bottom of the crypt, then one would have to expect a certain retardation rather than earlier appearance. The position of the last wave of labelled mitoses in Fig. 1 is therefore, at present, an unresolved issue.

A further problem which should be considered is a possible influence of diurnal fluctuations of the mitotic index on the FLM curves in Fig. 1. Published reports on such diurnal variations of the mitotic index and labelling index in the crypt cells are contradictory. Some authors were unable to find diurnal variations (Bullough, 1948; Leblond & Stevens, 1948; Bertalanffy, 1960; Pilgrim *et al.*, 1963, 1965) other authors have reported some degree of variations (Sigdestad *et al.*, 1969; Sigdestad & Lesher, 1971, 1972; Scheving *et al.*, 1972; Al-Dewachi *et al.*, 1976; Potten *et al.*, 1977). If there were diurnal variations of the mitotic and labelling indices in the jejunal crypt cells of the mouse they could not be due to periodic shifts of the duration of the G_1 -phase or S-phase, since this would have to lead to time shifts in some of the FLM curves observed in the present work. No such shifts have been found; in fact one obtains exactly the same generation times whether one compares waves (3) and (1) or waves (4) and (2). However, diurnal fluctuations of the mitotic and labelling index could also be due to periodic changes in the transition rate of proliferating cells into the non-proliferating differentiated state; this would be in agreement with findings by Grube *et al.* (1970) for epidermal cells of the mouse. In this case no variations of cycle phase durations occur and therefore the FLM curves should remain unaffected. Thus, even if there were diurnal variations in the mitotic and labelling index in the crypt cells they could be disregarded in the present analysis.

Table 3 is a compilation from the work of various authors of mean durations of the cycle and the individual phases for cells of the jejunum of the mouse. The table contains data for all three sections of the small intestine. According to Lesher *et al.* (1961) there are no regional differences of cycle duration between the three sections of intestine. The data obtained in the present work for the epithelial cells in the jejunum of the mouse agree well with the values which have been obtained by other workers and with our own earlier data (Schultze *et al.*, 1972).

The FLM method in its modified form that has been applied in the present study leads to a substantially increased precision in the determination of the mean transit times through the individual phases of the cycle. Furthermore, it provides essential information on the *variances* of these transit times. The first important result in this connexion is the experimental

confirmation of the additivity of variances that corresponds to the lack of correlation of transit times through consecutive phases. One cannot with certainty conclude from the lack of correlation that the transit times are independently distributed. In principle, there could be negative and positive interdependence that happen to cancel and result in zero correlation. Nevertheless the observed absence of correlation is, at least for the jejunal crypt cells, an important support of a theoretical assumption which had up to now been a somewhat doubtful element in the established mathematical treatment of FLM curves. A second more general conclusion can be drawn. Fig. 3 shows that there is substantial proportionality between the variances σ_i^2 of the observed waves of labelled mitoses and the mean transit times \bar{t}_i . This implies that the variance of the transit time through a particular phase of the cycle is proportional to the mean duration of this phase. In other words, equal phase age intervals correspond to equal increments of the variance of the transit time. One concludes that the different phases of the cycle are subject to a similar degree of statistical fluctuations in cell progression. In particular, this applies also to the S-phase in comparison to the rest of the cycle.

From the slope of the straight line in Fig. 3 one obtains the relation between the mean duration \bar{t} of a phase age interval and the corresponding variance σ^2 .

$$\sigma^2 = 0.29 \text{ hr} \cdot \bar{t} \quad (7)$$

The variances that result according to this equation for the individual phases of the cycle differ slightly from the ones which are calculated directly; in Table 2 they have been listed in brackets.

Little information exists in the literature on the variances of the transit times of crypt epithelial cells through the phases of the cycle. However, Al-Dewachi *et al.* (1975) report the coefficients of variation of the transit times which were obtained by evaluating a single label FLM curve according to the computer method of Gilbert (1972). These coefficients of variation, i.e. the ratios of the standard deviations and the mean transit times were 0.21, and 0.15, respectively, for the whole cycle C and for $G_2 + S$. This compares to the values 0.15, and 0.19 which can be derived from Table 2. From the values given by Al-Dewachi *et al.* (1975) one obtains a coefficient of variation of 0.63 for G_1 phase, this compares to the much smaller value 0.3 given in Table 2. If the earlier results were valid one would have to conclude that progress of the cells through G_1 phase is subject to considerably larger fluctuations than the progress through the rest of the cell cycle. Our results contradict this finding, since equation (7) implies that the progress of the crypt epithelial cells through the cycle is subject to the same degree of randomness in the different phases.

ACKNOWLEDGMENTS

The authors gratefully acknowledge the skilful technical assistance of Mrs H. Hagenbusch and Mrs Ch. Oppmann. This work was supported by grants from the Deutsche Forschungsgemeinschaft, SFB 105.

REFERENCES

- AL-DEWACHI, H.S., WRIGHT, N.A., APPLETON, D.R. & WATSON, A.J. (1975) Cell population kinetics in the mouse jejunal crypt. *Virchows Arch. B Cell Path.* **18**, 225.
- AL-DEWACHI, H.S., WRIGHT, N.A., APPLETON, D.R. & WATSON, A.J. (1976) Studies on the mechanism of diurnal variation of proliferative indices in the small bowel mucosa of the rat. *Cell Tissue Kinet.* **9**, 459.

- ASHIHARA, T. (1973) Computer optimization of the fraction of labelled mitosis analysis using the fast fourier transform. *Cell Tissue Kinet.* **6**, 447.
- BERTALANFFY, F.D. (1960) Mitotic rates and renewal times of the digestive tract epithelia in the rat. *Acta anat.* **40**, 130.
- BROCKWELL, P.J., TRUCCO, E. & FRY, R.J.M. (1972) The determination of cell-cycle parameters from measurements of the fraction of labelled mitoses. *Bulletin of Math. Biophysics Chicago*, **34**, 1.
- BULLOUGH, W.S. (1948) Mitotic activity in the adult male mouse, *Mus musculus* L. The diurnal cycles and their relation to waking and sleeping. *Proc. Roy. Soc. B* **135**, 212.
- BURHOLT, D.R., SCHULTZE, B. & MAURER, W. (1973) Autoradiographic confirmation of the mitotic division of every mouse jejunal crypt cell labelled with [³H]thymidine. *Cell Tissue Kinet.* **6**, 229.
- CAIRNIE, A.B. LAMERTON, L.F. & STEEL, G.G. (1965) Cell proliferation studies in the intestinal epithelium of the rat. I. Determination of the kinetic parameters. *Exp. Cell Res.* **39**, 528.
- GILBERT, C.W. (1972) The labelled mitoses curve and the estimation of the parameters of the cell cycle. *Cell Tissue Kinet.* **5**, 53.
- GRUBE, D.D., AUERBACH, H. & BRUES, A.M. (1970) Diurnal variation in the labeling index of mouse epidermis: a double isotope autoradiographic demonstration of changing flow rates. *Cell Tissue Kinet.* **3**, 363.
- HARTMANN, N.R., GILBERT, C.W., JANSSON, B., MACDONALD, P.D.M., STEEL, G.G. & VALLERON, A.J. (1975) A comparison of computer methods for the analysis of fraction labelled mitoses curves. *Cell Tissue Kinet.* **8**, 119.
- KOVACS, L. & POTTEN, C.S. (1973) An estimation of proliferative population size in stomach, jejunum and colon of DBA-2 mice. *Cell Tissue Kinet.* **6**, 125.
- LEBLOND, C.P. & STEVENS, C.E. (1948) The constant renewal of the intestinal epithelium in the albino rat. *Anat. Rec.* **100**, 357.
- LESHER, S., FRY, R.J.M. & KOHN, H.I. (1961) Aging and the generation cycle of intestinal epithelial cells in the mouse. *Gerontologia*, **5**, 176.
- LESHER, S. & SACHER, G.A. (1968) Effects of age on cell proliferation in mouse duodenal crypts. *Exp. Geront.* **3**, 211.
- MAURER, W., SCHULTZE, B., SCHMEER, A.C. & HAACK, V. (1972) Autoradiographic studies on the mode of growth in jejunal crypt cells of the mouse. *J. Microsc.* **96**, 181.
- PILGRIM, C., ERB, W. & MAURER, W. (1963) Diurnal fluctuations in the numbers of DNA synthesizing nuclei in various mouse tissues. *Nature*, **199**, 863.
- PILGRIM, C., LENNARTZ, K.J., WEGENER, K., HOLLWEG, S. & MAURER, W. (1965) Autoradiographische Untersuchungen über tageszeitliche Schwankungen des ³H-Index und des Mitose-Index bei Zellarten der ausgewachsenen Maus, des Ratten-Fetus sowie bei Ascites-Tumorzellen. *Z. Zellforsch.* **68**, 138.
- POTTEN, C.S., AL-BAWARI, S.E., HUME, W.J. & SEARLE, J. (1977) Circadian rhythms of presumptive stem cells in three different epithelia of the mouse. *Cell Tissue Kinet.* **10**, 557.
- QASTLER, H. & SHERMAN, F.G. (1959) Cell population kinetics in the intestinal epithelium of the mouse. *Exp. Cell Res.* **17**, 420.
- SCHEVING, L.E., BURNS, E.R. & PAULY, J.E. (1972) Circadian rhythms in mitotic activity and 3-H-thymidine uptake in the duodenum: Effect of isoproterenol on the mitotic rhythm. *Am. J. Anat.* **135**, 311.
- SCHULTZE, B., HAACK, V., SCHMEER, A.C. & MAURER, W. (1972) Autoradiographic investigation on the cell kinetics of crypt epithelia in the jejunum of the mouse. *Cell Tissue Kinet.* **5**, 131.
- SCHULTZE, B., MAURER, W. & HAGENBUSCH, H. (1976) A two emulsion autoradiographic technique and the discrimination of the three different types of labelling after double labelling with ³H- and ¹⁴C-thymidine. *Cell Tissue Kinet.* **9**, 245.
- SIGDESTAD, C.P., BAUMAN, J. & LESHER, S.W. (1969) Diurnal fluctuations in the number of cells in mitosis and DNA synthesis in the jejunum of the mouse. *Exp. Cell Res.* **58**, 159.
- SIGDESTAD, C.P. & LESHER, S. (1971) Photo-reversal of the circadian rhythm in the proliferative activity of the mouse small intestine. *J. Cell Physiol.* **78**, 121.
- SIGDESTAD, C.P. & LESHER, S. (1972) Circadian rhythm in the cell cycle time of the mouse intestinal epithelium. *J. Interdiscipl. Cycle Res.* **3**, 39.
- STEEL, G.G. & HANES, S. (1971) The technique of labelled mitoses: Analysis by automatic curve-fitting. *Cell Tissue Kinet.* **4**, 93.
- TAKAHASHI, M., HOGG, J.D. JR. & MENDELSON, M.L. (1971) The automatic analysis of FLM curves. *Cell Tissue Kinet.* **4**, 505.

APPENDIX

Relation between the FLM waves and the transit-time densities

All those cells are purely ^3H -labelled that leave S-phase during the time interval $\Delta L (= 2 \text{ hr})$ between ^3H - and ^{14}C -pulse labelling. All those cells are purely ^{14}C -labelled that enter S-phase during ΔL . It is convenient to refer to the middle of the interval ΔL as time $t = 0$. The mathematical relations need only be derived for the first wave of ^3H -labelled mitoses, as it will be apparent that the same relations apply to all other FLM waves.

Let ϕ be the cell flow per unit time. Then the number of purely ^3H -labelled cells that have left S-phase in the time interval t_L to $t_L + dt_L$ and have reached the midpoint of mitosis in the time interval t_M to $t_M + dt_M$ is:

$$\phi f_{G_2+M/2}(t_M - t_L) dt_M dt_L \quad (\text{A.1})$$

Accordingly the number of all those purely ^3H -labelled cells that have left S-phase during the time interval ΔL and that pass the midpoint of mitosis in the time interval $t - M/2$ to $t + M/2$ is equal to:

$$\phi \int_{-\Delta L/2}^{\Delta L/2} \left[\int_{t-M/2}^{t+M/2} f_{G_2+M/2}(t_M - t_L) dt_M \right] dt_L \quad (\text{A.2})$$

With the assumption of a fixed duration M of mitosis this is equal to the number of purely ^3H -labelled cells in mitosis at time t . The total number of cells in mitosis is ϕM , therefore the fraction of labelled mitoses at time t is:

$$f_1(t) = \frac{1}{M} \int_{-\Delta L/2}^{\Delta L/2} \int_{t-M/2}^{t+M/2} f_{G_2+M/2}(t_M - t_L) dt_M dt_L \quad (\text{A.3})$$

One can readily see that this may also be written in the form:

$$f_1(t) = \Delta L f_{G_2+M/2}(t) * w_L(t) * w_M(t) \quad (\text{A.4})$$

where the stars designate the operation of convolution and where the auxiliary functions $w_L(t)$ and $w_M(t)$ are defined as:

$$w_L(t) = \begin{cases} \frac{1}{\Delta L} & \text{for } -\frac{\Delta L}{2} < t < \frac{\Delta L}{2} \\ 0 & \text{otherwise} \end{cases} \quad \text{and} \quad w_M(t) = \begin{cases} \frac{1}{M} & \text{for } -\frac{M}{2} < t < \frac{M}{2} \\ 0 & \text{otherwise} \end{cases} \quad (\text{A.5})$$

Equation (4) gives the relation between the ideal transit time distribution and the observed FLM wave. It expresses the fact that the observed FLM wave differs from the ideal transit time distribution in two ways. First, the area under the FLM wave is not unity but is equal to the time interval ΔL between ^3H - and ^{14}C -labelling; secondly, the shape of the transit time distribution is distorted by a convolution with the two box-shaped functions $w_L(t)$ and $w_M(t)$ that have the width ΔL and M , respectively. The relation is an approximation, insofar as the cells in mitosis at time t are taken to be identical with the cells that pass the midpoint of mitosis in the time interval $t - M/2$ to $t + M/2$.

In a convolution the mean values and the variances of the individual functions are additive. The two functions $w_L(t)$ and $w_M(t)$ have the mean values 0 and the variances $\Delta L^2/12$ and $M^2/12$, respectively. Accordingly one obtains the following two relations which permit the derivation of the mean value t_1 and the variance σ_1^2 of the underlying transit time distribution from the observed FLM wave:

$$t_1 = \bar{t}_{G2} + \frac{M}{2} = \frac{1}{A_1} \int_0^{\infty} t f_1(t) dt \tag{A.6}$$

where A_1 is the area under the FLM wave that is, as seen from Table 1, close to its theoretical value $\Delta L = 2$ hr

$$\sigma_1^2 = \sigma_{G2}^2 = \frac{1}{A_1} \int_0^{\infty} (t - t_1)^2 f_1(t) dt - 0.3 \text{ hr}^2 \tag{A.7}$$

where the correction term 0.3 hr^2 is equal to $(\Delta L^2 + M^2)/2$.

Analogous formulae apply to the other FLM waves. In the case of the first FLM wave, which has here been chosen as example, the variance σ_1^2 is small compared to the correction term, and its value is therefore subject to considerable uncertainty. This is not the case for waves 2, 3, and 4.

According to equations (A.6) and (A.7) the values \bar{t}_i and σ_i^2 listed in Table 1 have been obtained by straightforward numerical integrations over the observed FLM waves.